HAYATI
Journal of Biosciences

Vol. 31 No. 6, November 2024 1190-1200
DOI:10.4308/hjb.31.6.1190-1200
ISSN: 1978-3019
EISSN: 2086-4094

Water Monitor Lizard (*Varanus salvator*) Skin Microstructure: Histochemical and Morphometrical Studies of Fiber Type Characteristics (Histochemistry Fiber Skin Water Monitor)

Andhika Yudha Prawira[1*], Ni Luh Putu Rischa Phadmacanty[1], Gono Semiadi[2], Hellen Kurniati[2], Wahyu Trilaksono[2], Yulianto[1], Nurhidayat[3], Srihadi Agungpriyono[3]

[1]*Research Center for Applied Zoology, Research Organization for Life Science and Environment, National Research and Innovation Agency (BRIN), Cibinong, Bogor 16911, Indonesia*
[2]*Research Center for Biosystematics and Evolution, Research Organization for Life Science and Environment, National Research and Innovation Agency (BRIN), Cibinong, Bogor 16911, Indonesia*
[3]*Division of Anatomy Histology Embryology, School of Veterinary Medicine and Biomedical Science, Bogor Agricultural University, Bogor 16680, Indonesia*

ARTICLE INFO

Article history:
Received January 18, 2024
Received in revised form March 30, 2024
Accepted August 22, 2024

KEYWORDS:
elastin,
leather,
skin,
structure,
thick fiber,
thin fiber

ABSTRACT

Global demand for the water monitor's skin, *Varanus salvator*, has made it a valuable wildlife commodity. Leathercraft manufacturing must consider not only beauty but also the strength and flexibility of the leather, which is determined by its structure in the skin. Therefore, this study analyzed and evaluated the fiber type characteristic of the water monitor's skin. Skin samples were collected from 10 Sumatra water monitors with a Snout-Vent Length size of 39-89 cm and were divided into small (39-59 cm) and large (60-89 cm) groups. The skins from the dorsocervical, lumbosacral, and ventral regions were proceeded for histological sections. Histochemical approaches utilized were Hematoxylin Eosin, Picrosirius Red, and Elastin Verhoeff's Hematoxylin staining methods. Thick fibers are the main component in the skin, ranging from 69-73%, respectively, while thin fibers varied greatly and were observed predominantly in the reticular dermis. Fiber size in the reticular dermis of small lizards was lower than that of larger ones. Elastic fibers were observed abundantly at the border of the reticular dermis and subcutaneous layer in both small and large lizards. Moreover, the skin of the small-sized lizard also has a lower morphometric than that of a large-sized lizard, both in thickness and fiber type percentage. Therefore, the skin of small-sized lizards was considered less tough than that of large-sized lizards.

1. Introduction

The demand for water monitor lizard, *Varanus salvator*, has increased in the international leather market. The raw leather found in the lizard, specifically from the islands of Borneo and Sumatra, Indonesia, is particularly desirable for exporters compared to those from Java (Nijman 2016; Boscha *et al.* 2020). Consequently, the water monitor lizard in Sumatera is widely exploited to meet the international trade demand, while the meat and other remaining body parts are considered waste (Arida *et al.* 2020). Although the Indonesian government does not protect this species, it is included in Appendices II of The Convention on International Trade in Endangered Species (CITES) (Menteri Perdagangan 2013; CITES 2023). It is categorized as least concern (LC) based on the International Union for Conservation of Nature (IUCN) red list (Quah *et al.* 2021).

Leathercraft manufacturing must consider not only beauty and delicacy but also the leather's strength, durability, and flexibility, which are determined by its structure (Boonchuay *et al.* 2018). The skin structure consists of two main layers, the epidermis, and the dermis. The epidermis offers protection from water and acts as a barrier, while the dermis contains various appendages, including hair, eyelashes, feathers, and glands, as well as other tissues such as nerves and blood vessels. In addition, the dermis provides suppleness, firmness,

* Corresponding Author
E-mail Address: andh007@brin.go.id

and elasticity to the skin through an extracellular matrix composed of collagen fibers, microfibrils, and elastic fibers embedded in hyaluronic acid and proteoglycans (Breitkreutz *et al.* 2009). The dermal connective tissue is the largest component of the skin and consists of fibrous and non-fibrous components. Meanwhile, the connective tissue's composition determines the skin's properties and characteristics. Connective tissues such as collagen, elastin (fibrous components), proteoglycans, and glycoproteins (non-fibrous components) are involved in skin firmness, pressure, elasticity, flexibility, and viscosity (Kent & Carr 2001; Akers & Denbow 2008). The arrangement and composition of collagen determine skin toughness, hence, the greater the amount of collagen in the extracellular matrix, the stronger the skin (Survana *et al.* 2013).

A previous study by Bonchuay *et al.* (2018) provided insights into the skin's general structure and cytokeratin properties in different areas of the water monitor lizard skin, including the epidermis and dermis. The thickness of the dermis ranged from 562-856 µm, with the thinnest on the ventral side and the thickest on the dorsal neck. Superficial fibers were also smaller than deep ones. However, this study did not further examine the types of fibers found in the skin. In addition, differences between body size groups were also not analyzed. This is important because the age and body size of the monitor lizard skin determine the optimal harvest age for obtaining high-quality skin. In general, the most common harvested monitor lizard for skin production had 56.50±6.40 cm in SVL (Snout Vent Length) and 3.55±1.55 kg in body weight (Boscha *et al.* 2020). A water monitor lizard of this size is often preferred due to its minimal scarring and relatively soft skin. Conversely, those with larger sizes are less desirable because they are considered to have many scars, which reduce skin quality (Setyawatiningsih 2018).

No study has established a correlation between fiber characteristics and various body sizes of monitor lizard skins. Therefore, this study was conducted to characterize the fibers in the skin of the water monitor lizard at various body sizes to determine the fundamental differences affecting skin quality as a leather industry product.

2. Materials and Methods

2.1. Animals

This experimental study used skin samples from 10 water monitor lizards obtained from a slaughterhouse in Palembang, Sumatra, Indonesia. The skin was taken from the lizard with SVL (Snout Vent Length) of small (39-59 cm, N = 5) and large (60-89 cm, N = 5) groups. The area of specimen collection was the dorsocervical (N = 9; small = 4, large = 5), lumbosacral (N = 10; small = 5, large = 5), and ventral (N = 10; small = 5, large = 5) regions, respectively. Additionally, ethical clearance was obtained from the National Research and Innovation Agency (BRIN) Republic of Indonesia no. 022/KE.02/SK/9/2022.

2.2. Histological Preparation

The skin samples were fixed in a 10% Buffered Neutral Formalin solution for 2 × 24 hours, transferred to 70% ethanol solution, and then processed for histological sections through dehydration step in serial concentration of ethanol from 80-100%, clearing in serial of xylene, and then embedded in the paraffin. The tissues were serially sectioned at 8 µm thickness to observe collagen fibers. The sections were dewaxed in xylene, rehydrated in serial concentration of ethanol (100-70%), and aquadest, then stained with Hematoxylin & Eosin (HE), Picrosirius Red (PSR), as well as Elastin Verhoeff's Hematoxylin - light green staining methods. The HE staining was conducted by treating the dewaxed sections in Mayer's Hematoxylin for 1 min followed by washing in a running tap for 5 min. The sample was further stained with Eosin for 2 min and then dehydrated in graded ethanol, cleared in xylene, and mounted with Entellan™.

Meanwhile, the PSR staining was performed by treating the dewaxed sections with 0.1% PSR for 60 min at room temperature and acid water (acetic acid 1%). The sections were dehydrated in three changes of ethanol, cleared in xylene, and mounted with Entellan™ (Junqueira *et al.* 1979a; 1979b). The Elastin Verhoeff's Hematoxylin – Light Green staining method was conducted by treating the dewaxed sections with Verhoeff's Hematoxylin for 30 min, then rinsed quickly in tap water, and differentiated in 2% ferric chloride. The sections were subsequently treated in sodium

thiosulfate for 5 min, washed in running tap water for 3 min, and counterstained with light green in acetic acid 1% for 30 sec, followed by dehydration in ethanol (2 changes; 30 sec – 1 min each), clearing in xylene (2 changes; 30 sec – 1 min each), and mounting with Entellan™ (Percival and Radi 2016). Afterward, the staining results were viewed under a microscope (IScope 1153-EPL, Euromex, Holland) at 10x and 40x objective lens magnification. The observation under a polarized light filter was conducted using a modified microscope with two linear polarized filters according to Prawira *et al.* (2022) method.

2.3. Measurement of Fiber Histomorphometry and Identification of Elastin Fibers

Histomorphometry was used to analyze the thickness of the skin, the relative percentage of thick and thin fibers, and the fiber size of the skin. The thickness of the skin was measured in two skin parts, i.e., the scales and interscales. The measurements were performed using ImageJ® (Schneider *et al.* 2012) processing software. Three serial sections of each body region's skin of water monitor lizards were used in the thickness measurement.

The percentage of thick and thin fibers was calculated from the average percentage of red (thick fibers) and green color (thin fibers) coverage areas. This was observed using the PSR staining with polarized light filters. The measurements were performed using ImageJ®. The percentage of thick and thin fibers was measured by calculating the coverage of red and green areas in 10 fields of view at 40X objective lens magnification. The stained images were processed using ImageJ® and then converted into greyscale images in red, green, and blue (RGB) stack images. Afterward, red and green filters were selected, and contrast was adjusted to optimize the color conversion. The coverage area was measured on both filters, associated with thick and thin fibers.

In addition, the size of collagen fibers was measured in the reticular dermis. Fiber size was measured by measuring the diameter or thickness in longitudinal or transverse sections. There were 35-50 fibers in the reticular dermis for each region of the animal body, namely dorsocervical, lumbosacral, and ventral.

The elastin fibers were identified using preparations stained with the Elastin Verhoeff's Hematoxylin-light green staining method. Identification was carried out in the dorsocervical, lumbosacral, and ventral regions as well as the papillaris dermis, reticular dermis, and subcutaneous layer parts.

2.4. Scanning Electron Microscope (SEM) Observation

The preparation of the sample followed Goldstein *et al.* (1992) protocol. The skins were cut into 0.5 × 0.3 × 0.2 cm in size, then cleaned with cacodylate buffer for 2 hr and agitated in an ultrasonic cleaner for 5 min. The skins were put in 2.5% glutaraldehyde for 7 hr and fixed in 2% tannic acid overnight. Then, the skins were washed with caccodylate buffer for 4 × 5 min, continued by dehydrating in graded ethanol at room temperature, and dried with tert butanol for 2 × 10 min, then frozen at -10°C. Later, the skins were dried in a vacuum drier before being coated with gold and observed in SEM (High Vacuum Scanning Electron Microscope Quattro S, Thermoscientific, USA). Fiber characteristics were observed on 5.00 kV HV and 5000x magnification on papillaris dermis, reticularis dermis, and subcutaneous layer of each region (dorsocervical, lumbosacral, and ventral).

2.5. Data Analysis

The obtained data were analyzed descriptively and statistically using Minitab Ver. 19 software. Statistical analysis was performed using the general linear model (GLM) with body size group (SVL), body region, skin thickness, color percentage, and fiber size as the variables and with the significant level at $p<0.05$. The significant value proceeded to the Tukey pairwise comparison method to identify the significant differences in each variable. In addition, the dataset was prepared by sorting complete data, which contained the data of body size group (SVL), body region, skin thickness, color percentage, and fiber size ($N = 9$) for Principal Component Analysis (PCA) to reduce the dimensionality and identify the correlation between all parameters.

3. Results

In general, the microstructure of the skin was similar in all regions but the dorsocervical and lumbosacral regions exhibited more melanin pigment than ventral region (Figure 1). The dermis of water monitor skin consists of two layers, namely papillaris and reticular, as shown in Figure 2. Fibers in the papillaris dermis

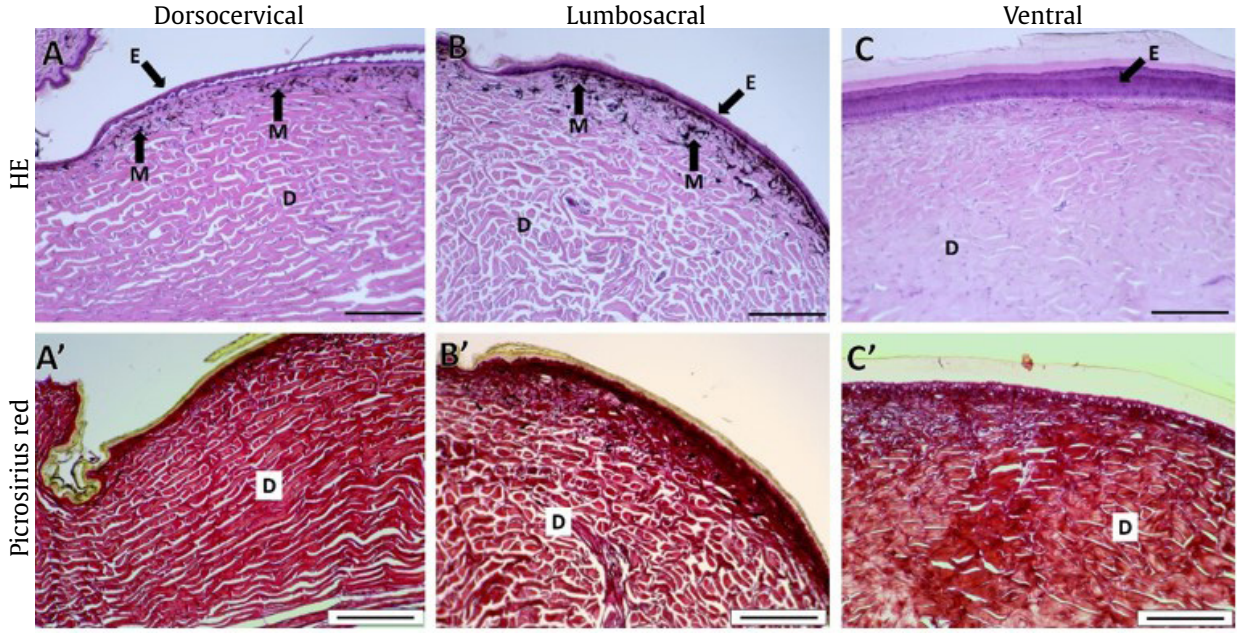

Figure 1. Histological image of skin microstructure of the water monitor lizard with HE staining (A, B, C) and Picrosirius red (A', B', C'). E: epidermis, D: dermis, M: melanin. (Scale bars: 200 µm)

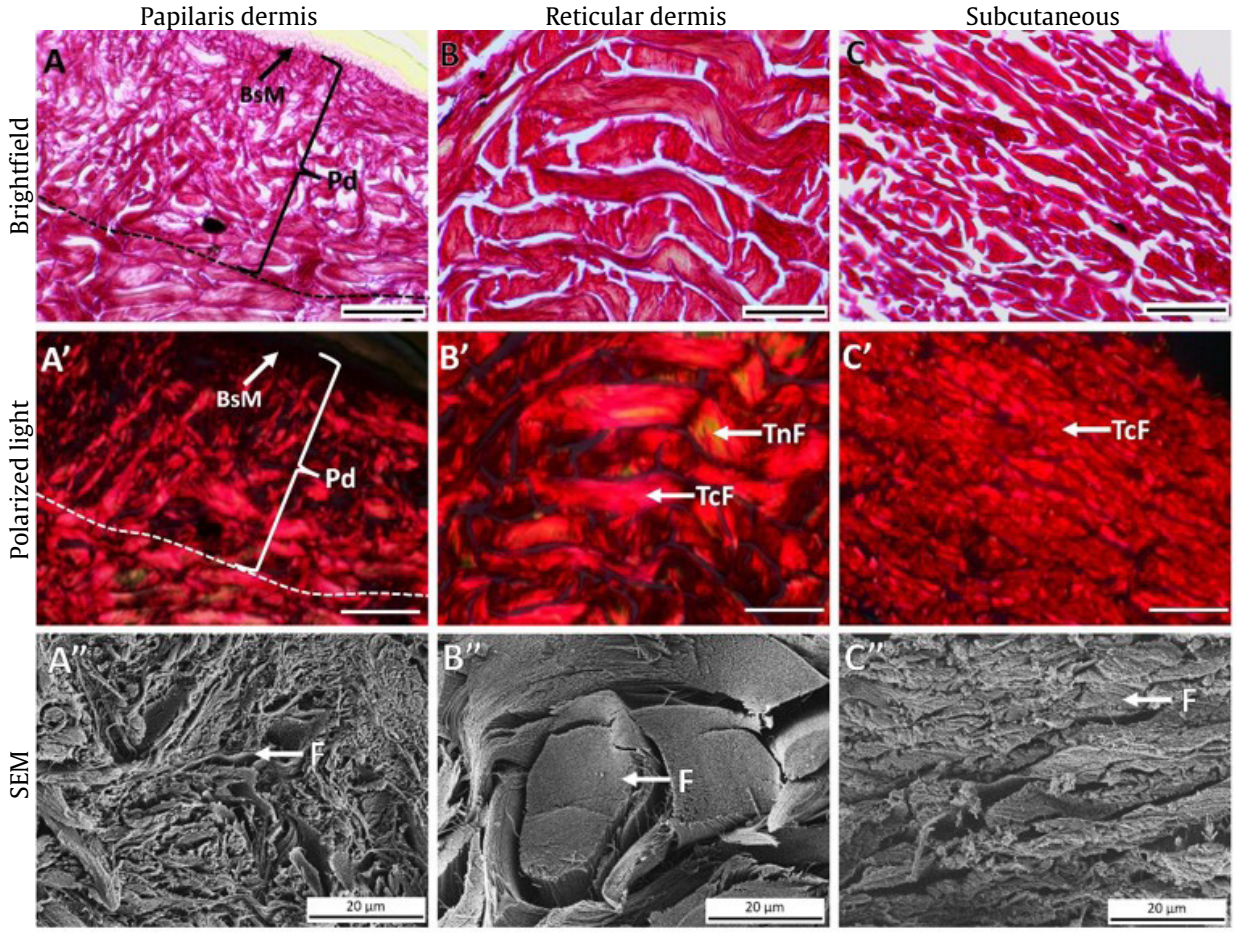

Figure 2. Picrosirius red staining of the skin of the water monitor lizard. The brightfield (A, B, C), under polarized light (A', B', C'), and ultrastructure under SEM (A", B", C"). The microstructure of skin part, i.e. papillaris dermis (A, A', A"), reticular dermis (B, B', B"), and subcutaneous layer (C, C', C"). The red-to-orange-yellow color in polarized light indicates the thick fiber (TcF), while the green color represents the thin fiber (TnF). BsM: basal membrane, F: collagen fiber, Pd: papillaris dermis, TcF: thick fiber, TnF: thin fiber. (Scale bars: 50 µm)

were composed of small, tight, arranged irregularly, and directly bordered with the epidermis. Although the fibers were small, almost all were thick, except for those in the basalis membrane, which were directly attached to the basal cells of the epidermis. These fibers appeared dark (non-polarized) due to the effect of polarizing light. The reticular dermis had large fibers arranged in a 3-way orientation, namely longitudinal, transverse, and vertical. They were predominantly composed of a mixture of thick and thin fibers. Furthermore, fibers in the subcutaneous layer were small-packed and more loosely organized compared to reticular dermis.

Generally, the histomorphometric of the water monitor's skin showed differences between small and large groups in skin thickness, fiber type percentage, and fiber size. The small-sized lizard had lower morphometric than large-sized lizard. The thickness of the skin in small-sized and large-sized was significantly different, with skin in the lumbosacral region of large-size water monitor lizards being the thickest (Table 1). The differences were observed both in the scale and interscale part.

Moreover, thick fibers in the dorsocervical and ventral regions were more numerous in the fiber type percentage than in the lumbosacral region. Meanwhile, the thin fibers observed varied greatly in all regions as shown by the mean and standard deviation of fiber percentage. According to the body size group, the small-sized lizard had the lowest percentage of thick fibers (red-orange color), while the large ones had the highest percentage. The small-sized lizard had the highest thin fibers percentage (green-yellowish color) compared to large ones. Still, this difference was not significant due to the high variation in the percentage of thin fibers. The fibers in the reticular dermis of the dorsocervical and ventral regions were larger than the lumbosacral region, while differences were also observed in the fiber between body size groups. The water monitor lizard with large body sizes had the largest fibers, while the smaller ones had the smallest fibers in the reticular dermis (Figure 3). Based on PCA analysis, the body size positively correlated with all the parameters (Figure 4), and the percentage of thick fiber showed the most closely related. The reticular fiber size was closely correlated to skin thickness.

The elasticity of the water monitor lizard skin was influenced by the distribution of elastin fibers. The results showed that the elastin fibers were predominantly distributed on the border of the reticular dermis and subcutaneous layer. In contrast, those in the reticular and papillaris dermis were significantly smaller and less abundant (Figure 5). This finding appears as a black line longitudinal across the skin. This characteristic was found in the skin with full and partly subcutaneous layers. The orientation of the elastin fibers was longitudinal and transversal in the subcutaneous layer. This characteristic was observed consistently in all regions and size groups, as shown in Figure 6.

Table 1. Histomophometric comparison of the water monitor's skin

Group SVL	Body region	Skin thickness (µm, mean±SD)		Color percentage (%, mean±SD)		Fiber size (µm, mean±SD)
		Scale	Interscale	Red	Green	Reticularis dermis
Small (39-59 cm)	Dorsocervical	938.08±153.30^{c}	427.78±118.43^{e}	70.75±6.49^{a}	2.76±2.67^{c}	10.89±2.43^{b}
	lumbosacral	1030.93±215.11^{c}	485.65±137.00^{e}	66.53±4.31^{b}	5.21±3.99^{c}	9.04±1.95^{c}
	Ventral	955.40±230.77^{c}	447.17±144.74^{e}	71.67±3.61^{a}	4.94±4.17^{c}	10.98±2.5^{b}
Average		972.26±208.05β	455.37±135.80γ	69.57±8.56β	4.41±5.10γ	10.26±2.31α
Large (60-89 cm)	Dorsocervical	1315.22±366.43^{b}	574.14±175.18^{d}	73.63±1.89^{a}	5.72±3.66^{c}	13.27±1.26^{a}
	lumbosacral	1595.30±404.82^{a}	669.21±227.07^{de}	72.51±1.79^{a}	5.42±3.80^{c}	10.78±1.6^{b}
	Ventral	1201.62±209.26^{b}	574.12±112.22^{de}	73.90±3.40^{a}	3.29±1.61^{c}	14.06±1.41^{a}
Average		1365.45±371.61α	611.65±189.10λ	73.35±5.38α	4.81±4.85γ	12.7±1.96β

Different font (a/b/c/d/e) among the value of each parameter column (skin thickness/color percentage/fiber size) indicates a significant difference at $p<0.05$

Different symbols (α/β/γ/λ) among the value in average of each parameter column (skin thickness/color percentage/fiber size) indicates a significant difference at $p<0.05$

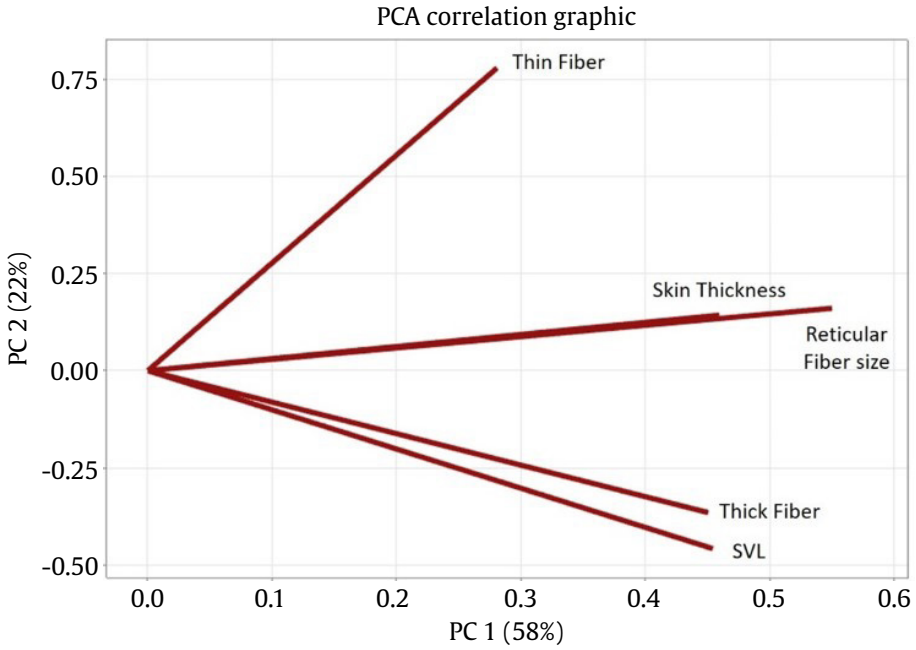

Figure 3. PCA Correlation Graphic of water monitor lizard

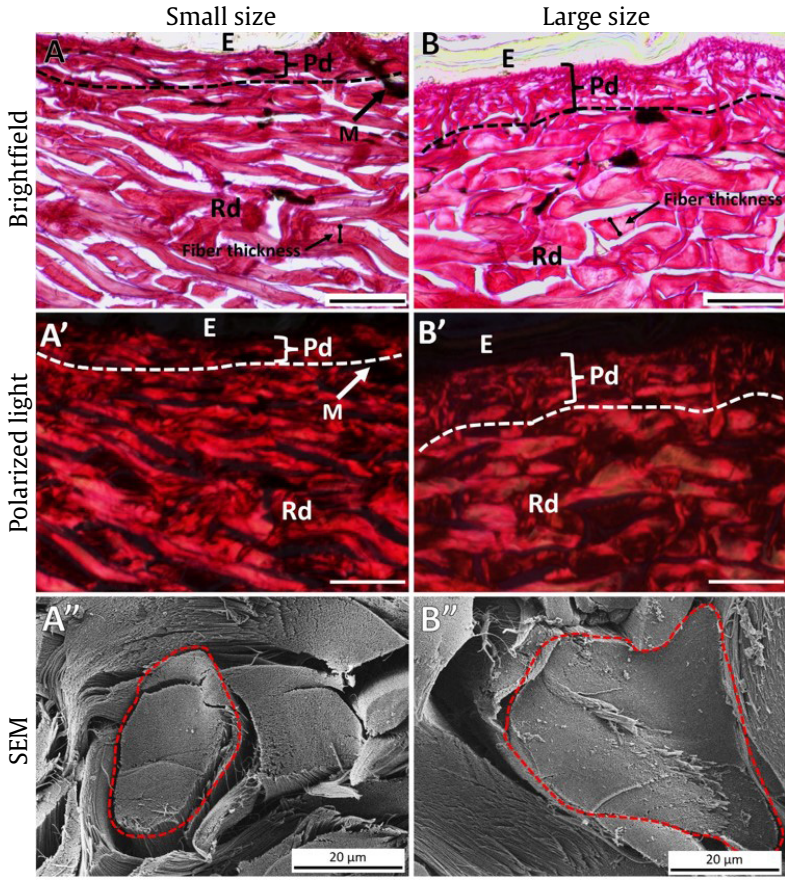

Figure 4. The microstructure comparison of the water monitor lizard skin between body sizes. The brightfield (A, B), under polarized light (A', B'), and under SEM (A", B"). The microstructure of the water monitor lizard skin with small body size (A, A') and large body size (B, B'). The comparison of the fiber thickness/diameter (red dash line) of reticular dermis in small size (A") and large size (B") lizard under SEM. E; epidermis, Pd: papillaris dermis, Rd: reticular dermis, M: melanin (Scale bars: 50 µm)

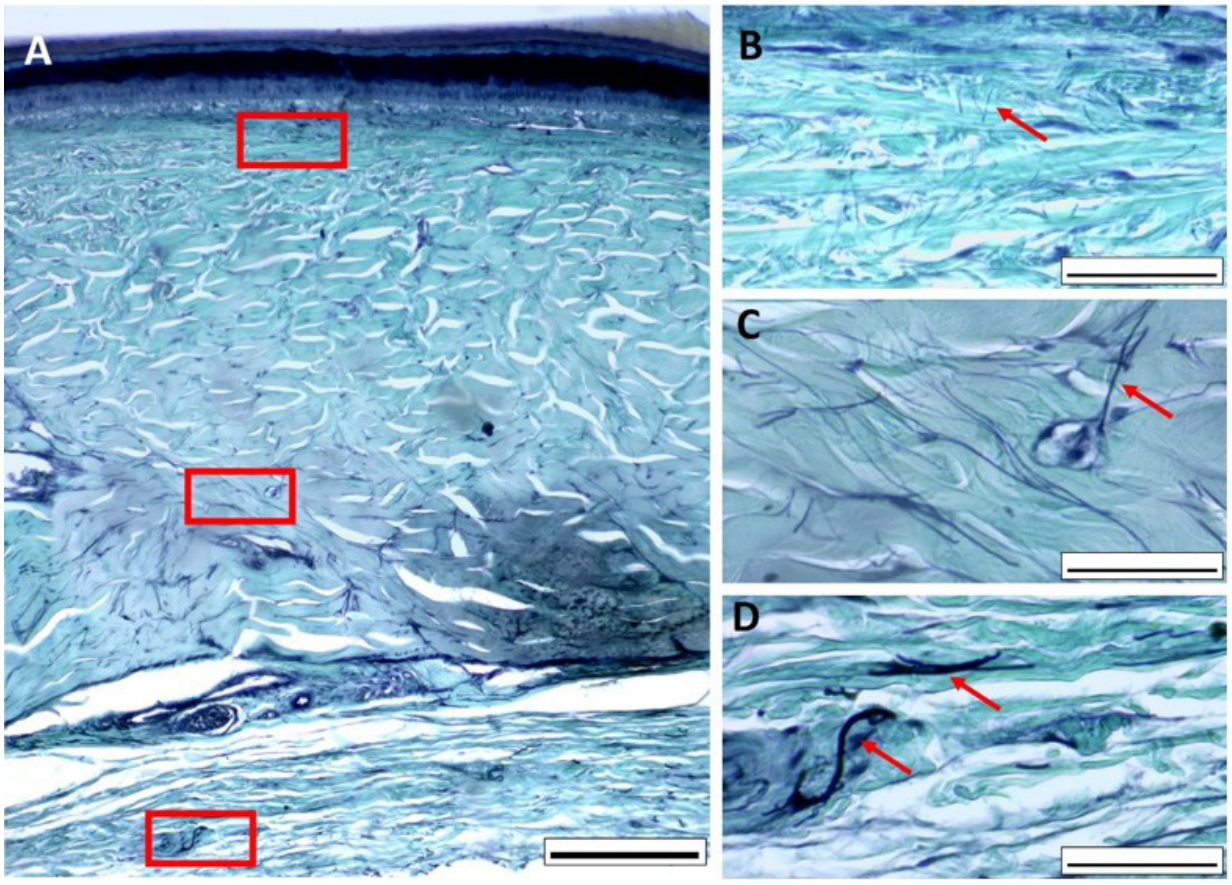

Figure 5. Elastic Verhoeff's Hematoxylin – light green staining of the water monitor lizard skin. Full thickness skin (A) and skin parts, papillaris dermis (B), reticular dermis (C), and subcutaneous layer (D). The elastic fiber was pointed by red arrow. The elastic fiber was prominent in the subcutaneous layer. (Scale Bar A: 200 µm; B, C, D: 50 µm)

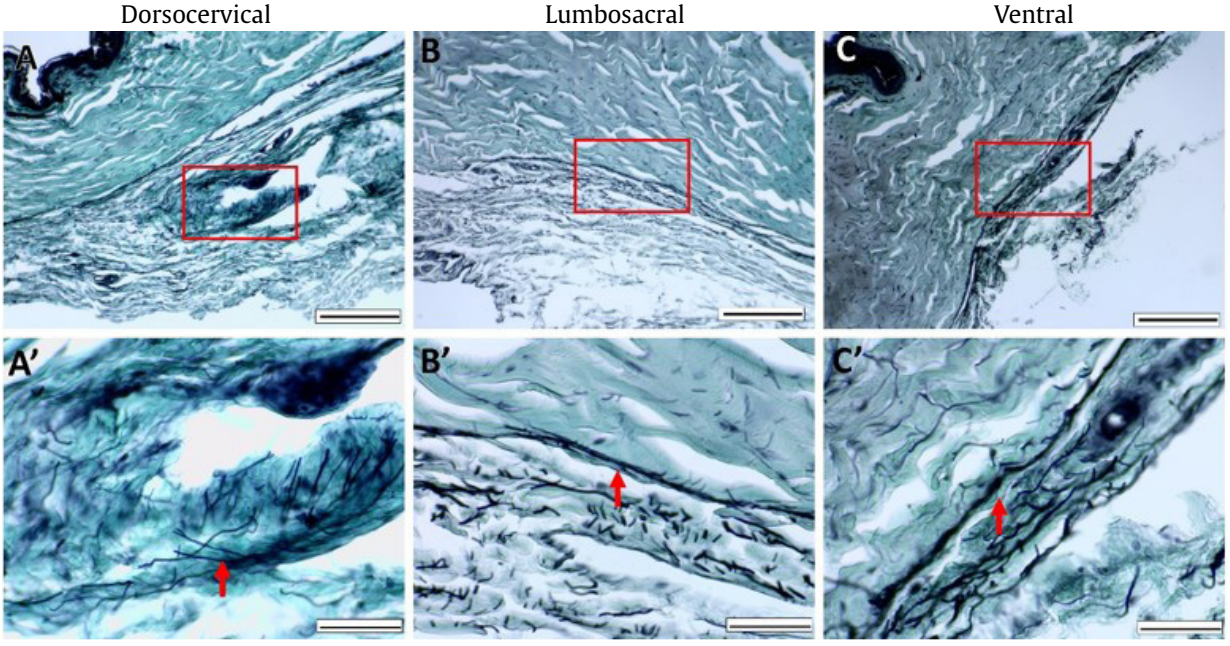

Figure 6. The prominent elastic fiber (red arrow) was found in the border of reticular dermis and subcutaneous layer in all regions of the body, i.e. dorsocervical (A, A'), lumbosacral (B, B'), and Ventral (C, C'). The higher magnification picture shown in A', B', and C'. (Scale bars A, B, C: 200 µm; A', B', C': 50 µm)

4. Discussion

The strength of raw and processed leather is influenced by three factors: the fiber type and cross-linking between the collagen fibrils, orientation, and the fibril diameter (Oxlund & Andreassen 1980; Wells *et al.* 2013). Collagen fibers play an important role in tissue structure and function, specifically for morphology, mechanical function, and wound healing at the organ level (Cowin 2000, 2004; Mosesson *et al.* 2001; Kjaer 2004; Lin *et al.* 2020). Type 1 collagen is the primary structural component of the skin that greatly affects its strength (Oxlund & Andreassen 1980). In addition, keratin, type III collagen, and elastin fibers also impact skin strength on a smaller scale (Oxlund & Andreassen 1980; Wells *et al.* 2013).

This study used a Histochemistry approach with picrosirius red staining to identify the distribution of thick and thin fibers, which can be associated with type I and III collagen. It has been used in several studies under polarized light to identify collagen types according to their colors (Binnebösel *et al.* 2010; Bayounis *et al.* 2011; Coen *et al.* 2013; Peeters *et al.* 2013; Cavallo *et al.* 2014). The results showed a strong yellow-red color associated with thick fibers (collagen type I), as well as a green color indicating thin fibers (collagen type III) (Junqueira *et al.* 1979a, 1979b). Although Lattouf *et al.* (2014) stated that picrosirius red staining was unable to differentiate collagen types due to color changes depending on the orientation of the collagen bundles, however we found that methods used in the study only stained the tissue section for 30 minutes, whereas the standard duration for picrosirius red staining is 60 minutes. Junquiera *et al.* (1979b) stated 30 min of staining with 0.1% picrosirius red is insufficient and should be doubled. Therefore, according to Lattouf *et al.* (2014) and Junqueira *et al.* (1979b), we differentiated the fiber in the skin into thick and thin fiber to identify different types of fiber-based on color in polarization light. These terms are also used in the study of Prawira *et al.* (2022) in the determination of fiber type in Sunda Porcupine. However, the picrosirius red staining can be used to measure the collagen content in normal and pathological tissue (Ejeil *et al.* 2003; Sansilvestri-Morel *et al.* 2007). Caetano *et al.* (2016) also demonstrated the comparability of the picrosirius red staining and quantified methods by measuring hydroxyproline and calculating the total fibrillar collagen in wound healing.

This study found thick fibers in the skin of the dorsocervical, lumbosacral, and ventral regions in the lizard measuring 39-89 cm SVL ranged from 69-73%. Differences in collagen percentage between regions were also found in Sunda porcupines (Prawira *et al.* 2022). Based on the results, the lizard with a large SVL size had a high percentage of thick fibers than those with a small SVL. This has implications on the skin's strength, which could be stronger in larger water monitor lizard, making it more difficult to transform into leather. Therefore, this might be one of the reasons why leather production favors small-sized water monitor lizards over large ones.

This study determined the orientation of collagen fibers in various parts of the skin, namely the papillaris, reticular, and subcutaneous layer. The arrangement was observed through histological observation with picrosirius red staining under polarized light. Based on the results, the fibers revealed a spectrum of colors depending on the size and packing density, indicating obvious collagen fiber orientation (Whittaker *et al.* 1994; Koren *et al.* 2001). The green-to-greenish-yellow color of thin and thick collagen fibers indicated that the collagen was loosely packed, while the orange-red color implied a dense package. The papillaris dermis exhibited a dense and irregular arrangement of fibers, while the reticular dermis was densely packed and consisted of at least three longitudinal, transverse, and vertical orientations. Under polarized light, the papillaris layer was red in color despite the small size of the fibers. On the other hand, the reticular layer had variations with a green-yellow color, indicating the presence of a thin or looser arrangement of fibers. In the subcutaneous layer, collagen fibers were more loosely arranged with smaller fibers than in the reticular dermis. These characteristics were similarly observed in all body regions and animal sizes.

The diameter of the fibers has been shown to have varying effects on leather strength in various animals. For example, in bovine leather, the fiber diameter significantly affected its strength, while in other leather such as goat, horse, pig, and sheep, no significant correlation was found (Wells *et al.* 2013). These characteristics can also be different among tissue types, such as in human aortic valves and tendons, wherein the strength of these tissues rises as the diameters of the type I collagen fibers increase (Michna 1984; Balguid *et al.* 2008; Biancalana Veloso & Gomes 2010). Based on the results of the present

study, the largest reticular dermis fiber size was found in the lizard with a large SVL. Consequently, the skin of the large-sized lizard is expected to be stronger than the smaller ones. The composition of type 1 collagen fibers and the smaller fiber size also affect the leather production process.

All biological tissues and materials are generally known to be visco-elastic (Li *et al.* 2009; Pissarenko *et al.* 2019). Therefore, skin properties are significantly determined by the structure of fiber bundles as well as elasticity and relaxation (Ehret & Itskov 2009; Pissarenko *et al.* 2019). In this study, elastin fibers were identified mainly in the border of reticularis dermis and subcutaneous layer, with orientations parallel to collagen fibers, which were longitudinal and transverse. Kielty (2006), stated that in general, elastin fibers consist of three types namely oxytalan at the dermo-epidermal junction, elaunin in the papillaris layer of the dermis, and thick elastin in the same position as the reticular layer. The quality of the final leather is significantly affected by elastin degradation, which improves properties such as softness, area yield, and evenness (Ornes *et al.* 1960; Alexander 1988). However, excessive elastin degradation causes looseness and increases mottling and veins in the final leather product (Lowe *et al.* 2000). Although in the water monitor's leather process, the subcutaneous layer is mostly separated from the skin along with other tissues that are attached to the skin (Shine *et al.* 1996), the elastin fiber in the border of the reticular dermis and subcutaneous layer could still be attached to the skin. The optimum separation of the subcutaneous layer in the "good side," both in dorsal or ventral cut, may be an important step in water monitor lizard's leather production. The abundant presence of elastin fibers in the subcutaneous layer could be a reference for exploring methods to improve skin quality by degrading elastin in this layer. Evaluating elastin fiber degradation in the leather production process can also help improve the quality of monitor lizard leather.

In conclusion, this study revealed differences in the distribution of fiber type in the skin of the water monitor lizard in both the body regions and sizes. The dorsocervical and ventral regions exhibited a higher percentage of thick fibers, indicating stronger and tougher skin than the lumbosacral region. The skin in the small water monitor lizard was composed of a lower amount of thick fiber compared to the larger ones, suggesting softer skin, which is easier to process. In addition, a significant amount of elastic fiber was found in the reticular dermis and subcutaneous layer border across all body regions and sizes.

Conflict of Interest

There is no confclict of interest, although partial funding was provided by the private sector AIRAI. Any decision regarding AIRAI's interest on water monitor lizard skin trading is within the jurisdiction of other institutions.

Acknowledgements

This study was partially funded by the Indonesian National Research and Innovation Agency (BRIN) funding scheme No. 9/III/HK/2022, "Rumah Program Pengungkapan Ancaman dan Dampak Perubahan Global Terhadap Status Ekosistem dan Biodiversitas Nusantara" to NLPRP, and No. 373/II/FR/3/2022, "Pendanaan Ekspedisi dan Eksplorasi" to GS. The Indonesian Reptile and Amphibian Trade Association (AIRAI) financially support for publication preparation through HK. The authors are grateful to CV. Berdikari Jaya, Palembang, Sumatera for the access to collect the samples.

References

Akers, R.M., Denbow, D.M., 2008. *Anatomy and Physiology of Domestic Animals*, first ed. Blackwell Publishing, Ames, Iowa.

Alexander, K.T.W., 1988. Enzymes in the tannery-catalysts for process. *Journal of The American Leather Chemists Association*. 83, 289–315

Arida, E., Hidayat, A., Mulyadi, M., Maireda, N. L., Subasli, D. R., Mumpuni, M., 2020. Consumption and trade of Asian Water Monitor, *Varanus salvator* as reliance on wildlife for livelihoods among rural communities in North Sumatra, Indonesia. *Journal of Tropical Ethnobiology*. 3, 81-92.

Balguid, A., Driessen, N.J., Mol, A., Schmitz, J.P., Verheyen, F., Bouten, C.V., Baaijens, F.P., 2008. Stress related collagen ultrastructure in human aortic valves—implications for tissue engineering. *Journal of Biomechanics*. 41, 2612-2617.

Bayounis, A.M., Alzoman, H.A., Jansen, J.A., Babay, N., 2011. Healing of peri-implant tissues after flapless and flapped implant installation. *Journal of Clinical Periodontology*. 38, 754-761.

Biancalana, A., Veloso, L., Gomes, L., 2010. Obesity affects collagen fibril diameter and mechanical properties of tendons in Zucker rats. *Connective Tissue Research*. 51, 171-178.

Binnebösel, M., Klink, C. D., Otto, J., Conze, J., Jansen, P.L., Anurov, M., Schumpelick, V., Junge, K., 2010. Impact of mesh positioning on foreign body reaction and collagenous ingrowth in a rabbit model of open incisional hernia repair. *Hernia*. 14, 71-77.

Boonchuay, D., Chantakru, S., Theerawatanasirikul, S., Pongchairerk, U., 2018. The anatomical study of water monitor (*Varanus salvator*) skin to apply for leatherwork production. *Veterinary Integrative Sciences*. 16, 53-68.

Boscha, E., Arida, E., Yudha, D.S., 2020. Dorsal colour patterns of Asian Water Monitor, *Varanus salvator* collected for trade in Cirebon, Indonesia. *Journal of Tropical Ethnobiology*. 3, 133-138.

Breitkreutz, D., Mirancea, N., Nischt, R., 2009. Basement membranes in skin: unique matrix structures with diverse functions?. *Histochemistry and Cell Biology*, 132, 1-10.

Caetano, G.F., Fronza, M., Leite, M.N., Gomes, A., Frade, M.A.C., 2016. Comparison of collagen content in skin wounds evaluated by biochemical assay and by computer-aided histomorphometric analysis. *Pharmaceutical Biology*. 54, 2555-2559.

Cavallo, J.A., Roma, A.A., Jasielec, M.S., Ousley, J., Creamer, J., Pichert, M.D., Baalman, S., Frisella, M.M., Matthews, B.D., Deeken, C.R., 2014. Remodeling characteristics and collagen distribution in synthetic mesh materials explanted from human subjects after abdominal wall reconstruction: an analysis of remodeling characteristics by patient risk factors and surgical site classifications. *Surgical Endoscopy*. 28, 1852-1865.

Coen, M., Menegatti, E., Salvi, F., Mascoli, F., Zamboni, P., Gabbiani, G., Bochaton-Piallat, M. L., 2013. Altered collagen expression in jugular veins in multiple sclerosis. *Cardiovascular Pathology*. 22, 33-38.

Cowin, S.C., 2000. How is a tissue built?. *J. Biomech. Eng.* 122, 553-569.

Cowin, S.C., 2004. Tissue growth and remodeling. *Annu. Rev. Biomed. Eng.* 6, 77-107.

Ehret, A.E., Itskov, M., 2009. Modeling of anisotropic softening phenomena: application to soft biological tissues. *International Journal of Plasticity*. 25, 901-919.

Ejeil, A.L., Gaultier, F., Igondjo-Tchen, S., Senni, K., Pellat, B., Godeau, G., Gogly, B., 2003. Are cytokines linked to collagen breakdown during periodontal disease progression?. *Journal of periodontology*. 74, 196-201.

Goldstein, J.I., Newbury, D.E., Echlin, P., Joy, D.C., Romig Jr, A.D., Lyman, C.E., Fiori, C., Lifchin, E., 1992. *Scanning Electron Microscopy and X-ray Microanalysis: a Text for Biologist, Materials Scientist, and Cytologists*, second ed, Plemun Press, New York.

Junqueira, L.C.U., Bignolas, G., Brentani, R.R., 1979a. A simple and sensitive method for the quantitative estimation of collagen. *Analytical Biochemistry*. 94, 96-99.

Junqueira, L.C.U., Bignolas, G., Brentani, R.R., 1979b. Picrosirius staining plus polarization microscopy, a specific method for collagen detection in tissue sections. *The Histochemical Journal*. 11, 447-455.

Kent, G.C., Carr, R. K., 2001. *Comparative Anatomy of the Vertebrates*, ninth ed. McGrawl-Hill Companies, New York.

Kielty, C.M., 2006. Elastic fibres in health and disease. *Expert Reviews in Molecular Medicine*. 8, 1-23.

Kjaer, M., 2004. Role of extracellular matrix in adaptation of tendon and skeletal muscle to mechanical loading. *Physiological Reviews*. 84, 649-698.

Koren, R., Yaniv, E., Kristt, D., Shvero, J., Veltman, V., Grushko, I., Feinmesser, R., Sulkes, J., Gal, R., 2001. Capsular collagen staining of follicular thyroid neoplasms by picrosirius red: role in differential diagnosis. *Acta Histochemica*. 103, 151-157.

Lattouf, R., Younes, R., Lutomski, D., Naaman, N., Godeau, G., Senni, K., Changotade, S., 2014. Picrosirius red staining: a useful tool to appraise collagen networks in normal and pathological tissues. *Journal of Histochemistry & Cytochemistry*. 62, 751-758.

Li, Z., Paudecerf, D., Yang, J., 2009. Mechanical behaviour of natural cow leather in tension. *Acta Mechanica Solida Sinica*. 22, 37-44.

Lin, J., Shi, Y., Men, Y., Wang, X., Ye, J., Zhang, C., 2020. Mechanical roles in formation of oriented collagen fibers. *Tissue Engineering Part B: Reviews*. 26, 116-128.

Lowe, E.K., Cooper, S.M., Passman, A., 2000. Measurement of elastin content in skin tissue and process liquors. *Journal of the Society of Leather Technologists and Chemists*. 84, 227-230.

Michna, H., 1984. Morphometric analysis of loading-induced changes in collagen-fibril populations in young tendons. *Cell and Tissue Research*. 236, 465-470.

Mosesson, M.W., Siebenlist, K.R., Meh, D.A., 2001. The structure and biological features of fibrinogen and fibrin. *Annals of the New York Academy of Sciences*. 936, 11-30.

Nijman, V., 2016. Perceptions of Sundanese men towards the consumption of water monitor lizard meat in West Java, Indonesia. *Biawak*. 10, 22-25.

Ornes, C.L., Roddy, W.T., Mellon, E.F., 1960. Study of the effect of the elastic tissue of hide on the physical properties of leather. *Journal of the American Leather Chemists Association*, 55, 600-621.

Oxlund, H., Andreassen, T.T., 1980. The roles of hyaluronic acid, collagen and elastin in the mechanical properties of connective tissues. *Journal of Anatomy*. 131, 611.

Menteri Perdagangan RI, 2013. Peraturan Menteri Perdagangan Republik Indonesia No. 50/M-DAG/PER/9/2013 tentang ketentuan ekspor tumbuhan alam dan satwa liar yang tidak dilindungi undangundang dan termasuk dalam daftar CITES. Jakarta, Indonesia.

Percival, K.R., Radi, Z.A. 2016. A modified *Verhoeff's elastin* histochemical stain to enable pulmonary arterial hypertension model characterization. *European Journal of Histochemistry*. 60, 2588.

Peeters, E., De Hertogh, G., Junge, K., Klinge, U., Miserez, M., 2013. Skin as marker for collagen type I/III ratio in abdominal wall fascia. *Hernia.* 18, 519–525.

Pissarenko, A., Yang, W., Quan, H., Brown, K. A., Williams, A., Proud, W.G., Meyers, M.A., 2019. Tensile behavior and structural characterization of pig dermis. *Acta Biomaterialia*, 86, 77-95.

Prawira, A.Y., Novelina, S., Farida, W.R., Darusman, H.S., Warita, K., Hosaka, Y.Z., Agungpriyono, S., 2022. Determination of thick and thin fibres distribution in Sunda porcupine dorsal skin (*Hystrix javanica*) using Picrosirius red staining. *Anatomia, Histologia, Embryologia*. 51, 666-673.

Quah, E., Lwin, K., Cota, M., Grismer, L., Neang, T., Wogan, G., McGuire, J., Wang, L., Rao, D.Q., Auliya, M., Koch, A., 2021. *Varanus salvato*r. The IUCN Red List of Threatened Species 2021: e. T178214A113138439.

Sansilvestri-Morel, P., Fioretti, F., Rupin, A., Senni, K., Fabiani, J.N., Godeau, G., Verbeuren, T.J., 2007. Comparison of extracellular matrix in skin and saphenous veins from patients with varicose veins: does the skin reflect venous matrix changes?. *Clinical Science*. 112, 229-239.

Schneider, C.A., Rasband, W.S., Eliceiri, K.W., 2012. NIH image to imageJ: 25 years of image analysis. *Nature Methods*. 9, 671-675.

Setyawatiningsih, S.C., 2018. The Indonesia's water monitor (*Varanus salvator*, Varanidae) trading. *Journal of Physics: Conference Series.* 1116, 052059.

Shine, R., Harlow, P.S., Keogh, J.S., 1996. Commercial harvesting of giant lizards: the biology of water monitors Varanus salvator in southern Sumatra. *Biological Conservation*. 77, 125-134.

Suvarna, S.K., Layton, C., Bancroft, J.D., 2013. *Bancroft's Theory and Practice of Histological Technique*, seventh ed. Churchill Livingstone, China.

[CITES] The Convention on International Trade in Endangered Species, 2023. Export quotas: *Varanus salvator*. Available at: https://cites.org/eng/resources/quotas/export_quotas?field_country_target_id=78&field_species_target_id=varanus+salvator&field_specimens_target_id=&field_date_value%5Bmin%5D=2000-01-01&field_date_value%5Bmax%5D=2023-12-31. [Date accesed: 23 May 2023]

Wells, H.C., Edmonds, R.L., Kirby, N., Hawley, A., Mudie, S.T., Haverkamp, R.G., 2013. Collagen fibril diameter and leather strength. *Journal of Agricultural and Food Chemistry*. 61, 11524-11531.

Whittaker, P., Kloner, R.A., Boughner, D.R., Pickering, J.G., 1994. Quantitative assessment of myocardial collagen with picrosirius red staining and circularly polarized light. *Basic Research in Cardiology*. 89, 397-410.